Analysing the impact of myopia on the Stiles-Crawford effect of the first kind using a digital micromirror device

Alessandra Carmichael Martins* and Brian Vohnsen

Advanced Optical Imaging Group, School of Physics, University College Dublin

*Corresponding author: alessandra.carmichaelmartins@ucd.ie

Keywords

Stiles-Crawford effect of the first kind

Cone photoreceptors

Digital Micromirror Device

Myopia

Axial length

Abstract

Purpose: Photoreceptor light acceptance is closely tied to the Stiles-Crawford effect of the first kind (SCE-I). Whether the SCE-I plays a role in myopic development remains unclear although a reduction in directionality has been predicted for high myopia. The purpose of this study is to analyse the relationship between foveal SCE-I directionality, axial length, and defocus for emmetropic subjects wearing ophthalmic trial lenses during psychophysical measurements and for myopic subjects with their natural correction.

Method: A novel uniaxial flicker system has been implemented making use of a Digital Micromirror Device (DMD) to flicker between a 2.3 visual degrees circular reference and a set of circular test patterns in a monocular Maxwellian view at 1 Hz. The brightness of the test is adjusted by the duty cycle of the projected light to an upper limit of 22727 Hz. The wavelength and bandwidth are set by a tuneable liquid-crystal filter centred at 550 nm. A total of 4 measurement series for 11 pupil entrance points have been realized for the right eye of 5 emmetropic and 8 myopic subjects whose pupils were dilated with tropicamide. The emmetropic subjects wore ophthalmic trial lenses in the range of -3 to +9 dioptres to mimic hyperopic to highly myopic vision and resulting visibility plots have been fitted

to a Gaussian SCE-I function. In turn, the myopic subjects wore their natural correction during the analysis of the SCE-I. All subjects had their axial length determined with an ultrasound device.

Results: A SCE-I directionality parameter for well-corrected vision in the range of 0.03 to 0.06/mm^2 was found for the emmetropic subjects with corrected vision in fair agreement to values in the literature. The results also revealed a marked reduction in directionality in the range from 16% to 30% with every 3 dioptre increase of simulated myopia, as well as a 10% increased directionality in simulated hyperopic eyes. For both emmetropic and myopic subjects a decrease in directionality with axial length was found in agreement with theoretical expectations.

Conclusion: The study confirms a clear link between SCE-I directionality, uncorrected defocus, and axial length. This may play a role for emmetropization and thus myopic progression as cone photoreceptors capture light from a wider pupil area in elongated eyes due to a geometrical scaling.

1. Introduction

The Stiles-Crawford Effect of the first kind (SCE-I) describes a reduced visibility of light being obliquely incident on the retina[1] associated to the light interaction with cone photoreceptors.[2] This effect is more prominent as the stimulus enters closer to the pupil edge, diminishing the visual sensitivity to approximately a quarter of its maximum value when the pupil is large. The SCE-I is typically evaluated in a Maxwellian view by a subjective comparison between a reference field entering near the pupil centre, where visibility is maximized and, a test field, which scans the pupil vertically or horizontally. There are two common systems that have been used to measure this effect:

- Bipartite field system, in which a dual-path setup is used to visualize the reference and test fields side-by-side.[3,4] In this system, the shifting of the test field is achieved by rotating a beam splitter or half-mirror in the Fourier plane of the eye pupil.
- Flicker field system, where one field and the other are alternated at a given frequency.[1,5] This allows the system to be uniaxial, and therefore, eliminate unwanted displacements and spectral errors arising between the two paths of the previous system.[6] The authors have recently reported on the use of such a technique for direct analysis of the integrated SCE-I.[7]

In both cases, the brightness of the test field is adjusted until the visual similarity with the reference reigns, and the intensity ratio between them is determined.

The SCE-I is characterised by the visibility of the test field, η, relative to its position, r, from the pupil centre, which often fits well to a Gaussian function, as seen in Figure 1. Traditionally, this is expressed as:

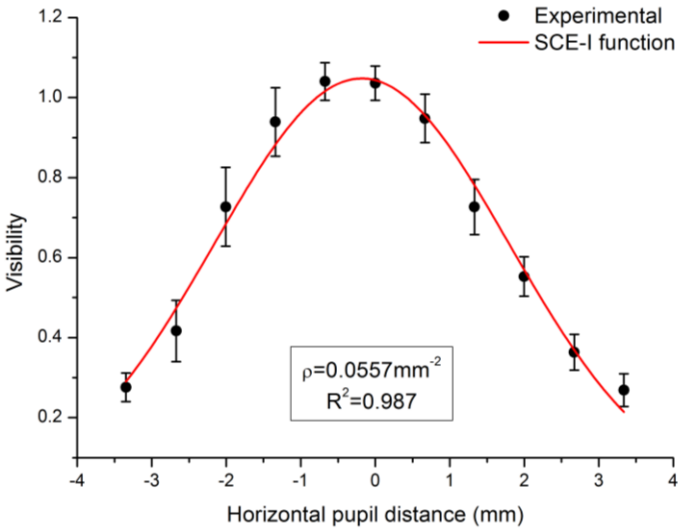

Figure 1: Measured visibility of the test field versus the pupil position at λ=550nm (Δλ=22nm) for one subject (AC) involving 4 horizontal scans across the pupil. Experimental values are fit to the Gaussian SCE-I function and error bars indicate ±1 standard deviation.

$$\eta = 10^{-\rho(\lambda)(r-r_0)^2} \quad (1)$$

where r_0 is the pupil position of maximum visibility, and $\rho(\lambda)$, is the directionality parameter which is wavelength dependent. The ρ-value commonly determined at the fovea is around 0.05mm^{-2}, although both subject and wavelength dependent.

The point of maximum visibility is located near the pupil centre, coinciding with the common pointing direction of the retinal cone photoreceptors. In the case of a myopic eye, the axial length is typically greater than that of an emmetropic eye[8], and therefore, the pointing direction of the foveal cones will likely be closer to the visual axis. A former study by Choi *et al*.[9] performed with emmetropes, moderate myopes and high myopes, analysed differences in both photoreceptor pointing direction and acceptance angles by looking at the peak position and shape factor of the SCE-I function respectively. The research reports a reduction in the directionality parameter across the retina with increasing myopia, although differences between moderate myopes (from -3D to -5D of refractive correction) and high myopes were found to be non-significant. The largest ρ-values were found for emmetropes.

Another study relating the SCE-I to myopia was carried out by Lochocki and Vohnsen[4], who suggested a geometric scaling relation to estimate the directionality parameter in accordance to the effective axial length and the dioptres of refractive correction for myopic subjects. Here, we consider two special cases namely that of (i) emmetropic subjects wearing trial lenses of different power (D) to mimic uncorrected myopia and that of (ii) myopic subjects with varying axial length, $L \simeq f_E + \Delta f$, wearing their natural correction during SCE-I characterization. For an idealized emmetropic eye $f_E = 22.2mm$, and Δf denotes a corrective term that accounts for any additional axial eye length of both emmetropic and myopic subjects. Cone photoreceptors are assumed to be aligned towards a common pupil point and geometrical scaling is used to relate the SCE-I directionality of an ideal emmetropic eye (ρ) to the directionality (ρ_M) of the (i) mimicked myopic eye and (ii) the refractive corrected myopic eye of increased axial length respectively. Both cases are shown schematically in Figure 2.

The ophthalmic trial lenses alter the angle of incidence on the retina due to the changed optical power of the emmetropic eye wearing a trial lens, whereas the corrected myopes with elongated axial length experience a reduced angle of incidence on the retina for the same pupil entrance point as an emmetrope. To a first approximation it can be shown that:

$$\rho_M \simeq (1 + 2Df_E)\rho \quad (2)$$

when mimicking myopia with trial lenses ($D < 0$) for an emmetropic eye. It should be stressed though that when mimicking uncorrected myopia there will be a slight shift of the light across the retina as a function of pupil entrance point (see Figure 2(a)). In turn, axial elongation ($\Delta f > 0$) of the corrected myopic eye leads to the following relationship (see Figure 2(b)):

$$\rho_M \simeq \left(1 - 2\frac{\Delta f}{f_E}\right)\rho \quad . \tag{3}$$

For the elongated myopic eye the angle of incidence on the retina is less than for an emmetropic eye for the same pupil entrance point. Thus, to achieve the same visibility the entrance point for the myopic eye would relocate further away from the pupil centre.

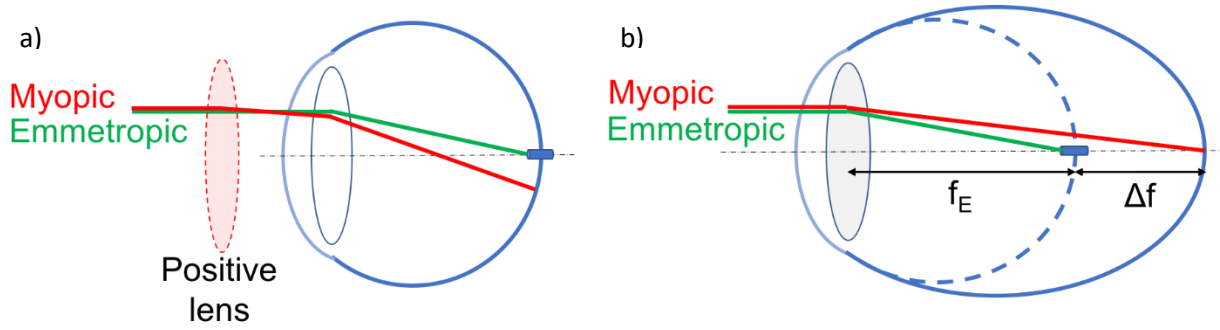

Figure 2: Schematic of the geometrical optics approach assuming a) emmetropic 22.2mm axial length eye mimicking myopia with a positive trial lens in front of the eye, and b) a refractive corrected myopic eye with increasing axial length and thus a correspondingly smaller angle of incidence of light onto the retina for the same pupil entrance point as an emmetropic eye.

To gain further insight into the role that the SCE-I may play on the progression of myopia, a set of ophthalmic trial lenses ranging between -3 dioptres for a slightly hyperopic perception, up to +9 dioptres for a highly myopic viewpoint are used to mimic this visual impediment. The measured values of the directionality in this case are compared to those obtained by equation 2. Additionally, the relation between the axial length measured with an ultrasound device (PalmScan A-2000), and the SCE-I for corrected myopic subjects is addressed and related to the directionality obtained by the geometrical model when a corrected myopic eye is considered.

In this study, a Digital Micromirror Device (DMD) is used in an automated uniaxial flicker system to characterize the SCE-I. We determine the effective directionality parameter for emmetropes while mimicking the impact of myopia and compare it to directionality values found for myopic subjects. The unique design in conjunction with the DMD endorses the removal of mechanical components

throughout the system, reducing vibrations and enhancing accuracy. Recent studies in retinal imaging have also used DMDs as an integrated illumination and scanning element for confocal imaging[10,11] and single pixel imaging[12,13] in ophthalmoscopes.

The paper is organized in four sections. Following this introduction, section 2 describes the experimental design and methodology followed to carry out the measurements. The results are included in section 3, where first, the role of defocus by mimicking myopia with trial lenses on 5 emmetropic subjects is presented, and second, the axial length dependence on the directionality for the same emmetropes and an additional 8 myopic subjects is shown. The discussion of the results is included in section 4, terminating with the conclusion of this study.

2. Methods

Apparatus

A uniaxial flicker system has been devised using a DMD (Vialux™ V-7001 VIS). The DMD is composed of an array of 1024 x 768 micromirrors arranged in a rectangular manner and mounted on a hinged structure allowing them to rotate individually ± 12 degrees, thus, providing a binary on- and off-state respectively. Each mirror corresponds to a given pixel of a grayscale image which can be projected by redirecting light from the brighter pixels onto a common screen, and deflecting light away to give a darker appearance. The speed at which any mirror can switch between its states is determinant to provide a greater contrast, limiting at 22727Hz for black and white images. This variation is regulated by adjusting the time ratio between the on and off positions of the micromirrors, namely, the duty cycle. Therefore, more intense light is transmitted through the system for larger values of the duty cycle. The linear dependence of the intensity variation with the duty cycle can be observed in Figure 3, with a slope of 1.031 ± 0.005 and $R^2 = 0.9998$. The mirror pitch is $13.7\mu m$ providing an active area of $14.0 \times 10.5 mm^2$. Additionally, the DMD has a built-in RAM of 64Gbit capable of storing up to 87380 patterns, therefore allowing a rapid change between desired images and preventing the subject to appreciate the transition.

The optical system used in this study was built using a quartz halogen lamp with a multimode fibre bundle ($\mathrm{NA} = 0.22$) as source, an infrared cut-off filter and an achromatic doublet to illuminate the DMD with white light. A schematic of the setup can be observed in Figure 4 The DMD is programmed using LabVIEW™ to provide a circular reference beam and alternate at a speed of 1Hz with a series of test patterns which scan the pupil horizontally in a monocular Maxwellian view. The binary pattern projections are created using MATLAB™ and, in order to achieve the maximum frame rate, they are loaded onto the DMD's on-board memory beforehand.

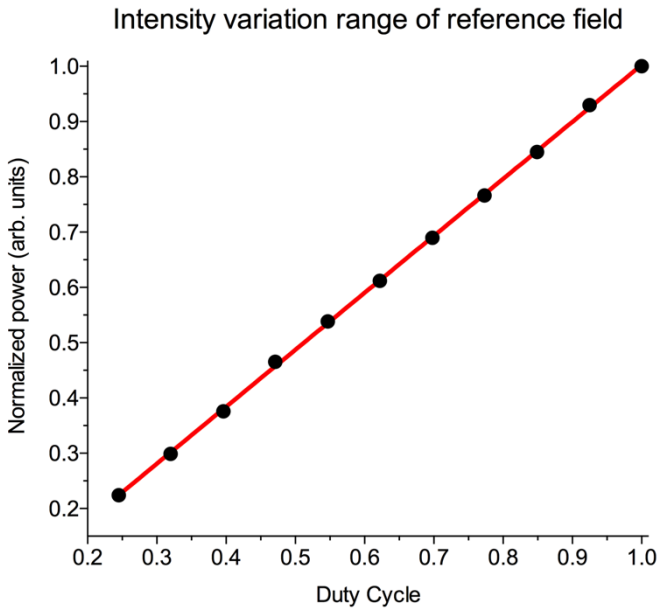

Figure 3: Measured dependence of the variation of the reflected beam intensity from the DMD in arbitrary units as a function of the duty cycle.

Firstly, these patterns are imaged onto a 20° circle top-hat diffuser by a set of two achromatic lenses. Light is then collected by a second set of achromatic lenses and reimaged, such that the diffuser is conjugated with the pupil plane. All together they complete a one-to-one optical system with the pupil plane. A Meadowlark™ selectable bandwidth tuneable filter is set to a bandwidth of 22nm centred at a wavelength of 550nm and placed before the last doublet lens. An iris is used to limit the area on the retina to 2.3 visual degrees. Additionally, infrared LEDs are used to illuminate the eye without disturbing the subject, while a beam splitter and camera are used to centre the subject's pupil by tracking the reflected light off the cornea.

A bright spot of 0.2mm or ~16-pixel diameter centred on the DMD, projected onto the diffuser and the pupil, is used as a reference, and the same-sized spot at different evenly spaced locations across the diagonal of the active area of the mirror array scans the pupil horizontally in such a way that the subject only sees the reference or the scanning light at any point in time. The duty cycle of the reference and test fields are controlled independently.

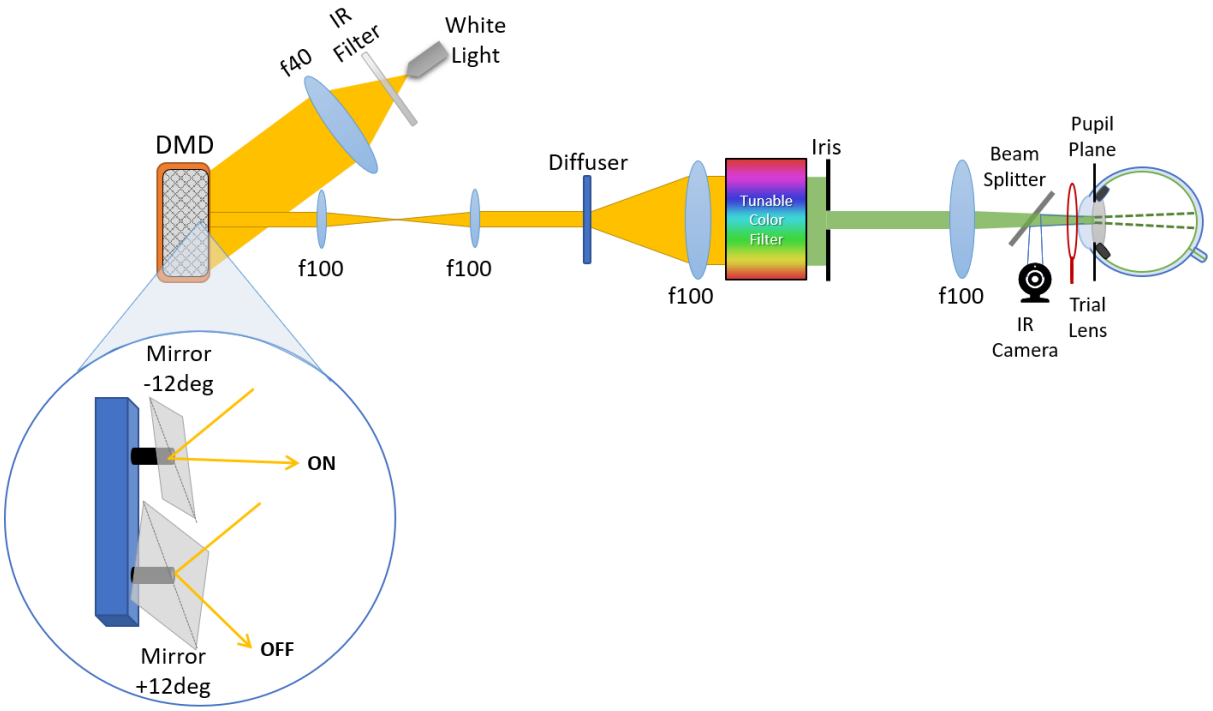

Figure 4: Schematic setup of a uniaxial flicker system to measure the SCE-I using a Digital Micromirror Device, which uses a binary switch of individual mirror pixels to deflect light. A 4f system is used to project a pattern onto the diffuser that is located at the conjugate plane of the pupil. A liquid-crystal tuneable colour filter sets the wavelength to 550nm and the iris determines the visual degrees in Maxwellian view.

Experimental procedure

To measure the SCE-I, the right pupil of all subjects was dilated, and accommodation was partially paralyzed with 1% tropicamide. A bite bar was used to reduce head and eye movement, and its position was adjusted along the X-Y-Z axes to ensure a good centring of the pupil to the reference beam at maximum visibility. Additionally, the two outermost test images along the horizontal line of the pupil were sequentially imaged to certify the best centration. A complete measurement consisted of 11 test patterns scanned across the horizontal line of the pupil and repeated 4 times to determine the standard deviation at each pupil position. The directionality parameter of the SCE-I was measured at the fovea by having each subject control the intensity of the test beam via a remote controller operated by the subject him/herself until the brightness matched that of the reference. At that point, the ratio between the duty cycles was recorded, and the next pupil-scanning-pattern on the DMD was projected at the push of a button. The relative visibility was then fitted to the Gaussian SCE-I function (Equation 1). All procedures were in accordance with the Declaration of Helsinki for experiments involving human subjects and approved by the Human Research Ethics Committee at University College Dublin. Specifications of all subjects taking part in this study are included in Table 1. The refractive errors were determined using an auto-refractor (EyeNetra^{TM}), and the axial lengths were

measured using an ultrasound biometer device (PalmScan A-2000 by Micro Medical Devices^{TM}). Two sets of measurements were realized:

Part 1. The directionality of 5 emmetropic subjects including the authors, whose refractive errors ranged between ±1D, were analysed while wearing trial lenses ranged between -3 and 9 dioptres, as well as their own refractive correction also through trial lenses.

Part 2. The directionality for all 13 subjects, 5 emmetropes and 8 myopes, with refractive errors ranging from +1 to -14D, was measured while wearing their personal spectacles when available, and the relation with their axial length was analysed.

3. Results

The directionality parameter of the SCE-I corresponding to 5 subjects using trial lenses of 3, 6 and 9 dioptres to mimic myopia have been plotted in Figure 5. An additional measurement using a -3 dioptre lens to mimic hyperopia has been included for verification purposes. The results show a negative slope of the SCE-I directionality parameter with increasing myopia, given that a clear reduction of the ρ-value is measured as the defocus is increased. For all five subjects here measured, approximately a 10% decrement is registered for the 3 dioptre increment between mimicked hyperopia and emmetropic vision, and a 16% is registered for the first 3 dioptre increase of mimicked myopia, which rises up to 30% per 3 dioptres between the last two trial lenses. The results of the ρ-value predicted by equation 2 for each degree of refractive correction is plotted on the same graph.

As mentioned, the refractive correction of a myopic subject is known to increase with the axial length of the eye, although the corneal curvature, in both central and peripheral regions, also plays a role.[14] Therefore, the refractive correction does not directly correlate to the axial length, as can be noted in Table 1, where the values of the axial lengths and refractive errors are presented for all subjects. To understand how the axial length can influence the directionality, the two measurements are plotted against each other in Figure 6, and approximated to a linear fit of slope -0.002mm^{-2} per *mm* axial length. Here, ρ-values were determined for all subjects while correcting vision with their personal spectacles.

Table 1: Axial lengths and spherical refractive corrections measured for the right eye of all subjects.

Subject	Age (yr.)	Axial Length (mm)	Refractive correction (D)
1 (AC)	27	22.45 ± 0.03	+1.00
2	27	22.81 ± 0.01	-0.75
3 (BV)	48	23.11 ± 0.05	0.00
4	31	23.40 ± 0.03	-0.75
5	33	23.81 ± 0.03	-1.00
6	49	24.20 ± 0.02	-4.50
7	22	25.13 ± 0.04	-4.00
8	23	25.16 ± 0.05	-3.75
9	35	26.73 ± 0.03	-6.50
10*	28	27.49 ± 0.03	-2.50
11	46	27.46 ± 0.05	-7.75
12	50	28.58 ± 0.25	-14.00
13	64	30.40 ± 0.46	-12.25

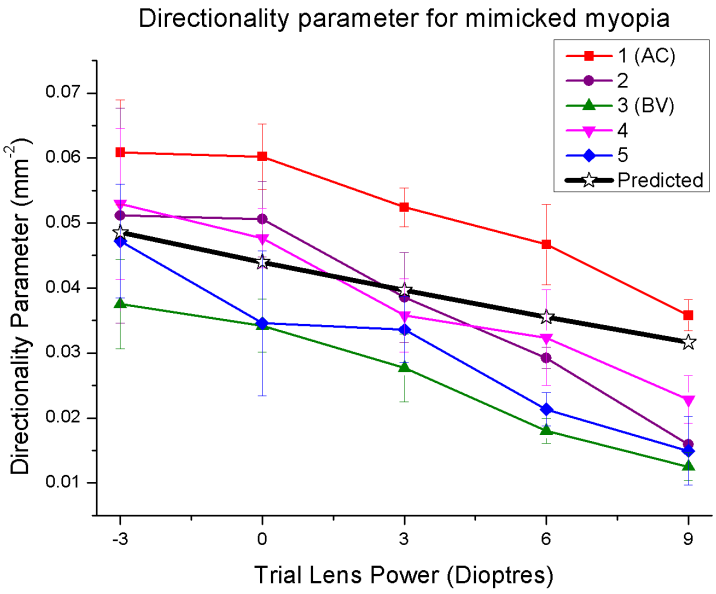

Figure 5: Plot of the directionality parameter values against the power of the trial lenses to mimic different degrees of myopia, and predicted ρ-values with the geometrical relation for different refractive corrections assuming a constant effective axial length. Error bars correspond to ±1 standard deviation.

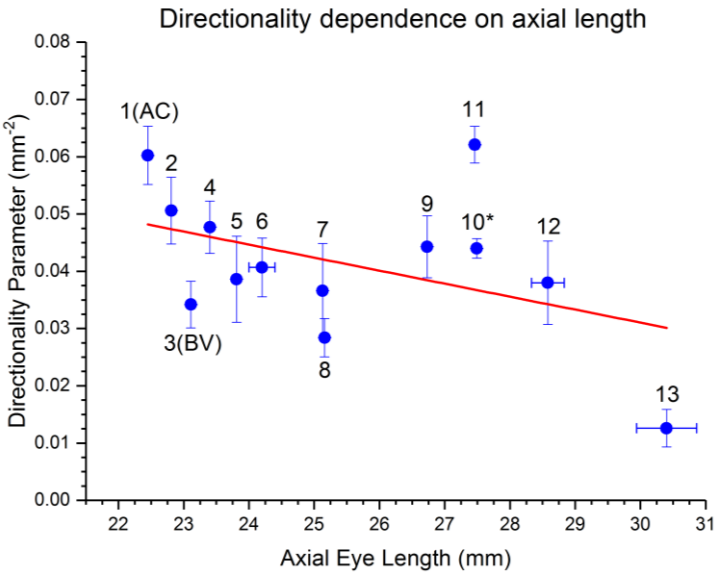

Figure 6: Plot representing the axial length of the right eye of the subjects against their directionality parameter, where error bars correspond to ±1 standard deviation. A linear fit of slope -0.0022 ± 0.0014 mm^{-2} per mm axial length is shown in red. The asterisk (*) denotes a subject who had LASIK surgery.

4. Discussion

In the first part of this study, the results presented in Figure 5 substantiates a distinct reduction in the directionality parameter of the SCE-I with the increase of defocus when mimicking myopia by use of ophthalmic trial lenses for emmetropic subjects. An initial 16% decrease for the first 3 dioptre increase (or 10% for hyperopia) of lens power is registered for all 5 subjects, which is in fair agreement to the geometrical relation in equation 2, that predicts a 10% reduction of the ρ-value for every 3D increase, assuming an effective axial length of 22.2mm. However, for higher powers of the lenses, the reduction rises to 20% and 30% consecutively for the following 3D increments. Although these exhibit a pronounced reduction, it must be taken into account that the axial length variations have not been considered in the geometrical relation and the translation of the test light at the retina for different pupil entrance points becomes increasingly problematic with higher optical power.

In the second part of the study, a slightly decreasing tendency in the directionality parameters are observed with larger axial eye lengths (plotted in Figure 6). For smaller axial length, the decreasing tendency is seen to be more pronounced, while as the elongation increases, this tendency is modestly lower on average. The subject marked with an asterisk had LASIK surgery to remove -5.5D of myopia 7 years before the measurements were taken. Given that the surgery does not affect the length of the eye and although a large axial length was registered, the anticipated drop in directionality could have been cut back. Subject 11 was the quickest in performing the measurements which could possibly

have impacted the results. Making use of equation 3, the slope can be written as: $slope = -\left(\frac{2}{f_E}\right)\rho$, and taking the values of f_E and ρ to be the average of that of the emmetropic subjects here considered, a theoretical slope of -0.0039mm^{-2} per *mm* of axial length, is obtained. Thus, both the theoretical and experimental slopes calculated are in fair agreement. Apart from the geometrical reduction in directionality with increasing axial length, an additional drop in directionality may be expected in case of cone disarray. This may be the case of subject #13 who showed a very low directionality. However, the fluctuations between subjects with large axial lengths are rather diverse, and therefore, further measurements involving a larger number of highly myopic subjects could offer better insight. Furthermore, noticeable differences between the shapes of plots representing the visibility and the radial pupil distance were observed for different subjects, ranging from a typical Gaussian, as seen in Figure 1, to those resembling a pulse function with rounded corners. As suggested by Rativa and Vohnsen[15], approximating the SCE-I results to a Super-Gaussian function, could in some instances provide a better fit and, thus, more accurate ρ-values. Finally, this study has introduced the DMD as a convenient tool for visual optic testing by allowing rapid changes of both pupil illumination patterns and brightness via the projection duty cycle.

5. Conclusion

Here, a novel uniaxial flicker system was presented using a DMD to measure the SCE-I and study the impact it may have on the progression of myopia. The DMD allows an extremely fast variation between Maxwellian views at different pupil position and a precise variation of their intensities, avoiding the use of mechanical components and providing a completely automated system. A clear link between the SCE-I directionality, uncorrected defocus, and axial length is confirmed. Myopia is mimicked using trial lenses ranging from -3 to +9D on emmetropes, thus providing insight on the impact of defocus. An increasing reduction opening at 16% has been registered for a 3D increase in mimicked myopia, which is in good agreement with the variation predicted by the geometrical relation between the directionality of emmetropic and myopic eyes. The role of the elongation of the axial length of the myopic eye has also been observed to modestly reduce the directionality in agreement with the theoretical expectations.

Disclosure

The authors report no conflicts of interest and have no proprietary interest in any of the materials mentioned in this article.

Acknowledgements

The authors would like to thank all the subjects who have participated in this study, and also, the financial support provided by the H2020 ITN MyFUN grant agreement No. 675137.

References

1. Stiles WS, Crawford BH. The luminous efficiency of rays entering the eye pupil at different points. Proc R Soc B. 1933;112:428–450.

2. Westheimer G. Directional sensitivity of the retina: 75 years of Stiles-Crawford effect. Proc R Soc B. 2008;275:2777–2786.

3. Lochocki B, Rativa D, Vohnsen B. Spatial and spectral characterisation of the first and second Stiles-Crawford effects using tuneable liquid-crystal filters. J Mod Opt. 2011;58:1817–1825.

4. Lochocki B, Vohnsen B. Defocus-corrected analysis of the foveal Stiles–Crawford effect of the first kind across the visible spectrum. J Opt. 2013;15:125301.

5. Stiles WS. The luminous efficiency of monochromatic rays entering the eye pupil at different points and a new colour effect. Proc R Soc B Biol Sci. 1937;123:90–118.

6. Vohnsen B. The retina and the Stiles–Crawford effects. In: Chapter 18 in: Handbook of Visual Optics Vol I, Ed P Artal. 2017. p. 257–276.

7. Vohnsen B, Carmichael A, Sharmin N, Qaysi S, Valente D. Volumetric integration model of the Stiles-Crawford effect of the first kind and its experimental verification. J Vis. 2017;(in press).

8. Wallman J, Gottlieb MD, Rajaram V, Fugate-Wentzek LA. Local retinal regions control local eye growth and myopia. Science. 1987;237:73–77.

9. Choi SS, Garner LF, Enoch JM. The relationship between the Stiles-Crawford effect of the first kind (SCE-I) and myopia. Ophthalmic Physiol Opt. 2003;23:465–472.

10. Muller MS, Elsner AE, Ozawa GY. Non-mydriatic confocal retinal imaging using a digital light projector. In: Manns F, Söderberg PG, Ho A, editors. 2013. p. 85670Y.

11. Vienola K V, Damodaran M, Braaf B, Vermeer KA, de Boer JF. Parallel line scanning ophthalmoscope for retinal imaging. Opt Lett. 2015;40:5335–5338.

12. Lochocki B, Gambín A, Manzanera S, Irles E, Tajahuerce E, Lancis J, et al. Single pixel camera ophthalmoscope. Optica. 2016;3:1056–1059.

13. Lochocki B, Gambín-Regadera A, Artal P. Performance evaluation of a two detector camera for real-time video. Appl Opt. 2016;55:10198.

14. Carney LG, Mainstone JC, Henderson B. Corneal topography and myopia. Invest Ophthalmol Vis Sci. 1997;38:311–320.

15. Rativa D, Vohnsen B. Single- and multimode characteristics of the foveal cones: the super-Gaussian function. J Mod Opt. 2011;58:1809–1816.